MEASUREMENTS OF FLUX DENSITIES AND GAIN CORRECTIONS AT 22485.1 MHZ

VLA TEST MEMORANDUM NO. 149

Patrick C. Crane

April 1987

The second run in the long-term program to monitor the flux densities of selected VLA calibrators occurred on 28-29 December 1985. The run included 1.3cm observations of the Baars' flux-density calibrators 3C48, 3C147, 3C286, and NGC 7027, plus the VLA calibrators 3C84 and 3C138. This memorandum will describe the analysis of these observations and present the flux densities and gain corrections obtained.

The amplitudes measured in such interferometric observations are subject to several effects:

DELAYS: The delays on the VLA are set with a tolerance of two nanoseconds, which corresponds to a reduction in amplitude of 1.4 percent. For the point and small sources observed in this program, this effect will be constant with time for each antenna, and the amplitude effects of small delay errors will still close.

SYSTEM TEMPERATURE: The system temperatures were measured continuously using the front-end synchronous detectors on each antenna. The CD preamplifier in antenna 23 was a specially designed cooled HEMT with a system temperature at the zenith of about 120 K, compared to 300-400 K for the cooled mixers on the other antennas and IFs. Consequently, the following analysis has been done for the C IFs only.

ATMOSPHERIC ATTENUATION: Fortunately, the weather during the observations was dominated by a stationary high-pressure system or "omega block" over the Southwest that diverted the jet stream and associated storm systems far north of the VLA. The atmosphere was uniformly dry and stable. George Martin's "TIPPER" procedure was run six times between the beginning and end of the twenty-four-hour run. The measured values of the zenith attenuation ranged between 0.032 and 0.040, and the mean value of 0.0358 +/- 0.0012 was used to correct the observations.

POINTING: The last VLA pointing run prior to our observations was on 17 December 1985. The pointing curves and residuals obtained were well behaved. The residuals were typically about 10" or 0.1 of the FWHM at 1.3cm. At this level, it was still desirable to observe in interferometer-pointing mode to measure the pointing offsets and determine corrections. Two problems arose from this decision: MODCOMP integration times longer than the standard 10 seconds (30 seconds for 3C84 and 50 seconds for the other sources) were needed for sensitivity, and as a consequence, the submode codes used to identify pointing positions were screwed up. The standard version of FILLER did not fill interferometer-pointing data and Barry Clark provided a special version to do so.

APERTURE EFFICENCY: As the elevation of a VLA antenna changes, its surface will deform. The deformations introduce phase variations across the aperture of the antenna that cause a loss of efficiency. According to Lee King, the surfaces of the VLA antennas were set to provide maximum efficiency at an elevation of 50 degrees. Lee's model of the structure of the VLA antennas predicts the rms errors and gain corrections given in Table 1.

Table 1. Predicted Rms Surface Errors and Corrections for VLA Antennas

ELEVATION (Degrees)	RMS ERROR (MM)	CORRECTION
0	0.305	1.086
10	0.254	1.059
20	0.203	1.037
30	0.140	1.018
40	0.076	1.005
50	0.000	1.000
60	0.076	1.052
70	0.152	1.021
80	0.254	1.059
90	0.330	1.102

FOCUS: The surface deformations also change the shape of the best-fit parabaloid and, consequently, the position of the focus. The corresponding focus curve has not been modeled nor measured, and the default values of the longitudinal foci were used throughout the observations.

SOURCE STRUCTURE: Except for 3C84 the sources observed are resolved at 1.3cm, even in the D array. Table 2 lists the uvlimits used in obtaining the ANTSOL solutions.

Table 2. Uvlimits Used for ANTSOL Solutions

SOURCE	UVLIMITS
3C48	0-3000nsec
3C84	None
3C138	0-2000nsec
3C147	0-2000nsec
3C286	0-8000nsec
N7027	0- 200nsec

As will be discussed below, because N7027 is so heavily resolved, the ANTSOL solutions were used only to determine pointing corrections.

ANALYSIS

The analysis of the data proceeded as follows: The special FILLER was used to fill all data, including that at 1.3cm, into the DEC-10. DBCON was used to place the 1.3cm data into its own database. The nominal pointing sequence followed in interferometer pointing is to integrate for one integration period at five nomimal positions - on, +0.5 HPBW in elevation, -0.5 HPBW in elevation, +0.5 HPBW in azimuth, and -0.5 HPBW in azimuth - with single integration periods allowed to move between positions, with the cycle repeating until the end of the scan. Because of the longer MODCOMP integration times used, the starting point in this sequence varied from scan to scan; we allowed sufficient time in each scan to provide at least a complete sequence. Because the nominal pointing was pretty good, I could establish the pointing sequence from a column listing from LISTER. Having identified the proper sequence of data, I then ran ANTSOL on the data for each pointing position. In the end for each of the 51 scans, I obtained five ASCII disk files, each listing the ANTSOL solutions for one pointing position.

The next step in the analysis was to use the pointing observations to calculate amplitudes corrected for pointing errors using a Fortran program I wrote called AMP.FOR. The inputs for each scan are a scan number (used for subsequent bookkeeping), source name, elevation (obtained from scanheadings), and the names of the files containing the on, +elevation, -elevation, +azimuth, and -azimuth ANTSOL solutions. For each scan AMP.FOR read in the ANTSOL solutions for all antennas and used a parabolic-fitting routine to calculate the elevation and azimuth pointing offsets and the corresponding corrected peak amplitudes for each antenna. The average amplitudes and errors and the total pointing offsets were calculated, the amplitudes were corrected for atmospheric attenuation using the zenith attenuation derived above, and the results for each scan were written to files with extensions .PK, .EPK, and .TOF.

The first estimate of the gain-correction curves was obtained using the twelve scans of 3C286. The Baars' formula was used to extrapolate the flux density - 2.53 Jy - of 3C286 at 22485.1 MHz. The observed gain corrections were calculated by dividing this flux density by the observed amplitudes. The gain-correction curve for each antenna was calculated by fitting in a least-squared-error sense the observed corrections with Legendre polynomials of the first kind. Since theoretically the minimum of this curve is at an elevation of 50 degrees, I fit with Legendre polynomials with n=0-4 centered on that elevation rather 90 degrees; i.e., for $x = \cos(E+40)$,

$$P_0(x) = 1,$$

$$P_1(x) = x,$$

$$P_2(x) = (3x^2-1)/2,$$

$$P_3(x) = x(5x^2-3)/2,$$

$$P_4(x) = (35x^4-30x^2+3)/8.$$

I then applied this first estimate of the gain-correction curves to the eight observations of 3C84, ten observations of 3C147, eleven observations of 3C48, and four observations of 3C138 to obtain estimates of their flux densities at 22485.1 MHz. Using the Baars' flux density for 3C286 and the estimates of the flux densities of the other four sources, I used the 51 scans covering elevations between 14 and 116 (i.e., over the top) degrees to obtain a second estimate of the gain-correction curves. With such excellent coverage in elevation, I was able to identify discrepant measurements (in the end 51 of 1170 measurements) to flag out of subsequent calculations.

FLUX DENSITIES

After several iterations of this procedure, I obtained the final flux densities and formal errors given in Table 3 for all the sources except N7027. Because N7027 is well resolved, the original VLA data were used to determine its flux density: only data from the thirteen antennas with baselines shorter than 200 nsec (4, 6, 10, 11, 14, 15, 16, 17, 18, 21, 25, 26, 28) were used; they were corrected using GTBCOR for atmospheric attenuation and on an antenna and scan basis for pointing errors and gain variations. The data (shown in Figure 1) were then exported to a VAX and the AIPS routine UVFIT was used to determine the best-fit gaussian model for N7027; the total flux density is given in Table 2, and the dimensions of the gaussian are 6.62 +/- 0.05" x 5.51 +/- 0.06" extended at position angle -30.6 +/- 2.2 degrees.

Table 3. Flux Densities at 22485.1 MHz

SOURCE	OBSERVED	BAARS
3C48	1.28 0.01	1.10 0.04
3C84	41.32 0.25	
3C138	1.17 0.01	
3C147	1.83 0.01	1.68 0.06
3C286	2.52 0.01	2.53 0.09
N7027	5.67 0.02	5.85 0.56

GAIN CURVES

Figure 2 shows the gain-correction curves for the 26 antennas (all but 9 and 27) that were operational during our observations. The curves have been normalized to their values at an elevation of 50 degrees so that they can be plotted on a common scale and compared. It is apparent that the observed gain-correction curves differ very significantly from the model given in Table 1 and with each other. The only explanation I have, which probably explains only a fraction of the variations observed, is that the longitudinal foci are not tracked and variations in focus cause additional variations in gain. The coefficients and errors of the normalized gain curves are tabulated in Table 4.

The unnormalized gain curves and all measurements (including those subsequently rejected) for the individual antennas are shown in Figures 3-28; the characters for the five sources are 3C48 (+), 3C84 (*), 3C138 (o), 3C147 (x), and 3C286 (▫).

Table 4. Coefficients of Antenna Gain Curves

ANTENNA	C0	C1	C2	C3	C4
1	1.142	0.479	0.325	0.062	0.055
	0.042	0.106	0.134	0.106	0.082
2	1.133	0.013	0.259	-0.108	-0.009
	0.047	0.120	0.152	0.122	0.092
3	1.171	-0.318	0.320	-0.122	-0.029
	0.046	0.115	0.146	0.116	0.089
4	1.179	0.083	0.410	0.012	0.070
	0.058	0.145	0.185	0.148	0.113
5	1.136	-0.096	0.362	0.019	0.120
	0.042	0.105	0.132	0.105	0.081
6	1.113	0.158	0.283	-0.028	0.075
	0.034	0.087	0.109	0.087	0.069
7	1.273	-0.289	0.725	-0.101	0.240
	0.054	0.138	0.174	0.139	0.107
8	1.112	0.103	0.254	0.010	0.040
	0.039	0.097	0.125	0.097	0.079
10	1.381	0.413	0.902	0.232	0.188
	0.099	0.246	0.293	0.218	0.138
11	1.235	0.535	0.537	0.313	0.090
	0.049	0.121	0.151	0.118	0.089
12	1.191	-0.015	0.428	-0.067	0.061
	0.053	0.133	0.169	0.135	0.104
13	1.096	0.044	0.197	-0.046	0.006
	0.034	0.085	0.108	0.086	0.066
14	1.452	0.558	1.036	0.399	0.176
	0.061	0.152	0.189	0.148	0.112
15	1.094	-0.077	0.223	-0.116	0.046
	0.037	0.091	0.116	0.092	0.071
16	1.061	-0.131	0.163	-0.081	0.056
	0.055	0.137	0.172	0.136	0.104

17	1.254	0.455	0.685	0.260	0.237
	0.039	0.099	0.124	0.098	0.079
18	1.240	0.215	0.724	0.169	0.324
	0.115	0.284	0.328	0.235	0.130
19	1.313	0.169	0.772	0.113	0.195
	0.043	0.108	0.137	0.109	0.084
20	1.208	0.026	0.380	-0.116	-0.048
	0.042	0.104	0.151	0.104	0.083
21	1.099	0.057	0.169	-0.034	-0.038
	0.052	0.131	0.156	0.115	0.072
22	1.172	0.209	0.423	-0.020	0.106
	0.048	0.119	0.151	0.120	0.093
23	1.131	-0.095	0.263	-0.172	0.001
	0.042	0.106	0.134	0.107	0.081
24	1.143	0.127	0.325	0.044	0.051
	0.039	0.099	0.125	0.100	0.079
25	1.110	-0.068	0.236	-0.109	0.020
	0.037	0.093	0.117	0.093	0.074
26	1.100	-0.015	0.174	-0.112	-0.035
	0.046	0.115	0.145	0.116	0.090
28	1.109	-0.023	0.277	-0.083	0.079
	0.045	0.114	0.144	0.115	0.092

DISCUSSION

The observed gain curves have been implemented in a program on the DEC-10 called KCOR.FOR in the [13,66] area; an example of how run this program is given in the Appendix. For each elevation specified KCOR lists the gain corrections for all antennas except 9 and 27 (which were not measured), the corresponding voltage corrections specify for AMPFACTOR in GTBCOR, and the average voltage correction for AMPFACTOR if an array-averaged value is desired. Unfortunately, the corrections must still applied manually using GTBCOR.

I have probably overemphasized the variations in the observed gain curves. Examination of the coefficients and errors in Table 4 reveals that for most antennas coefficients C3 and C4 (and often C1) are not statistically significant. As the example in the Appendix shows, the uncertainty in the gain corrections are typically about ten percent. The differences between the observed gain curves and the model in Table 1 are real - the observed curves show much greater variations with elevation than expected.

Rick Perley and I will be repeating these measurements this spring in the D array. Four or five antennas in addition to antenna 23 will be equipped with new 1.3cm receivers in both polarizations with system temperatures of about 160 K; the improved sensitivity should allow better measurements. I will also find solutions for all IFs which will for consistency checks. Unfortunately, other improvements such as real-time pointing and tracking the longitudinal foci must wait for the new on-line control system; we hope they will be available for the following set observations, when all or nearly all antennas will have new 1.3cm receivers.

APPENDIX Sample Execution of the Program KCOR.FOR

```
.EXE KCOR[13,66]
TYPE IN NUMBER (<=20) OF ELEVATIONS DESIRED
2
TYPE IN VALUES OF ELEVATIONS DESIRED
25 75
1.3CM GAIN CORRECTIONS AND ERRORS AT  25.00 DEGREES ELEVATION BASED UPON
OBSERVATIONS OF 85DEC28

 1     1.2328    0.0845
 2     1.1272    0.0959
 3     1.0212    0.0921
 4     1.1021    0.1164
 5     0.9844    0.0837
 6     1.1157    0.0691
 7     0.9897    0.1098
 8     1.0860    0.0778
 9     1.0000    0.0000
10     1.2131    0.1872
11     1.1834    0.0959
12     1.1060    0.1065
13     1.0889    0.0681
14     1.2423    0.1199
15     1.0541    0.0731
16     0.9944    0.1093
17     1.1342    0.0784
18     1.0376    0.2117
19     1.1244    0.0866
20     1.1898    0.0834
21     1.1047    0.0994
22     1.1542    0.0955
23     1.1062    0.0847
24     1.0940    0.0791
25     1.0721    0.0740
26     1.1088    0.0919
27     1.0000    0.0000
28     1.0595    0.0911

AMPFACTORS TO ENTER IN GTBCOR

 1     1.1103
 2     1.0617
 3     1.0105
 4     1.0498
 5     0.9922
 6     1.0563
 7     0.9948
 8     1.0421
 9     1.0000
10     1.1014
11     1.0878
12     1.0517
```

13	1.0435
14	1.1146
15	1.0267
16	0.9972
17	1.0650
18	1.0186
19	1.0604
20	1.0908
21	1.0511
22	1.0743
23	1.0518
24	1.0459
25	1.0354
26	1.0530
27	1.0000
28	1.0293

AVERAGE AMPFACTOR TO ENTER IN GTBCOR 1.0506

1.3CM GAIN CORRECTIONS AND ERRORS AT 75.00 DEGREES ELEVATION BASED UPON OBSERVATIONS OF 85DEC28

1	0.8834	0.0845
2	1.0206	0.0959
3	1.1811	0.0921
4	1.0434	0.1164
5	1.0824	0.0837
6	0.9565	0.0691
7	1.1441	0.1098
8	1.0077	0.0778
9	1.0000	0.0000
10	1.0709	0.1872
11	1.0094	0.0959
12	1.0593	0.1065
13	1.0105	0.0681
14	1.1259	0.1199
15	1.0161	0.0731
16	1.0334	0.1093
17	0.9814	0.0784
18	1.0069	0.2117
19	1.0826	0.0866
20	1.0645	0.0834
21	1.0267	0.0994
22	0.9604	0.0955
23	1.0335	0.0847
24	1.0259	0.0791
25	1.0329	0.0740
26	1.0218	0.0919
27	1.0000	0.0000
28	1.0055	0.0911

AMPFACTORS TO ENTER IN GTBCOR

1	0.9399
2	1.0102
3	1.0868
4	1.0215
5	1.0404
6	0.9780
7	1.0696
8	1.0038
9	1.0000
10	1.0348
11	1.0047
12	1.0292
13	1.0052
14	1.0611
15	1.0080
16	1.0166
17	0.9907
18	1.0034
19	1.0405
20	1.0318
21	1.0133
22	0.9800
23	1.0166
24	1.0129
25	1.0163
26	1.0108
27	1.0000
28	1.0028

AVERAGE AMPFACTOR TO ENTER IN GTBCOR 1.0165

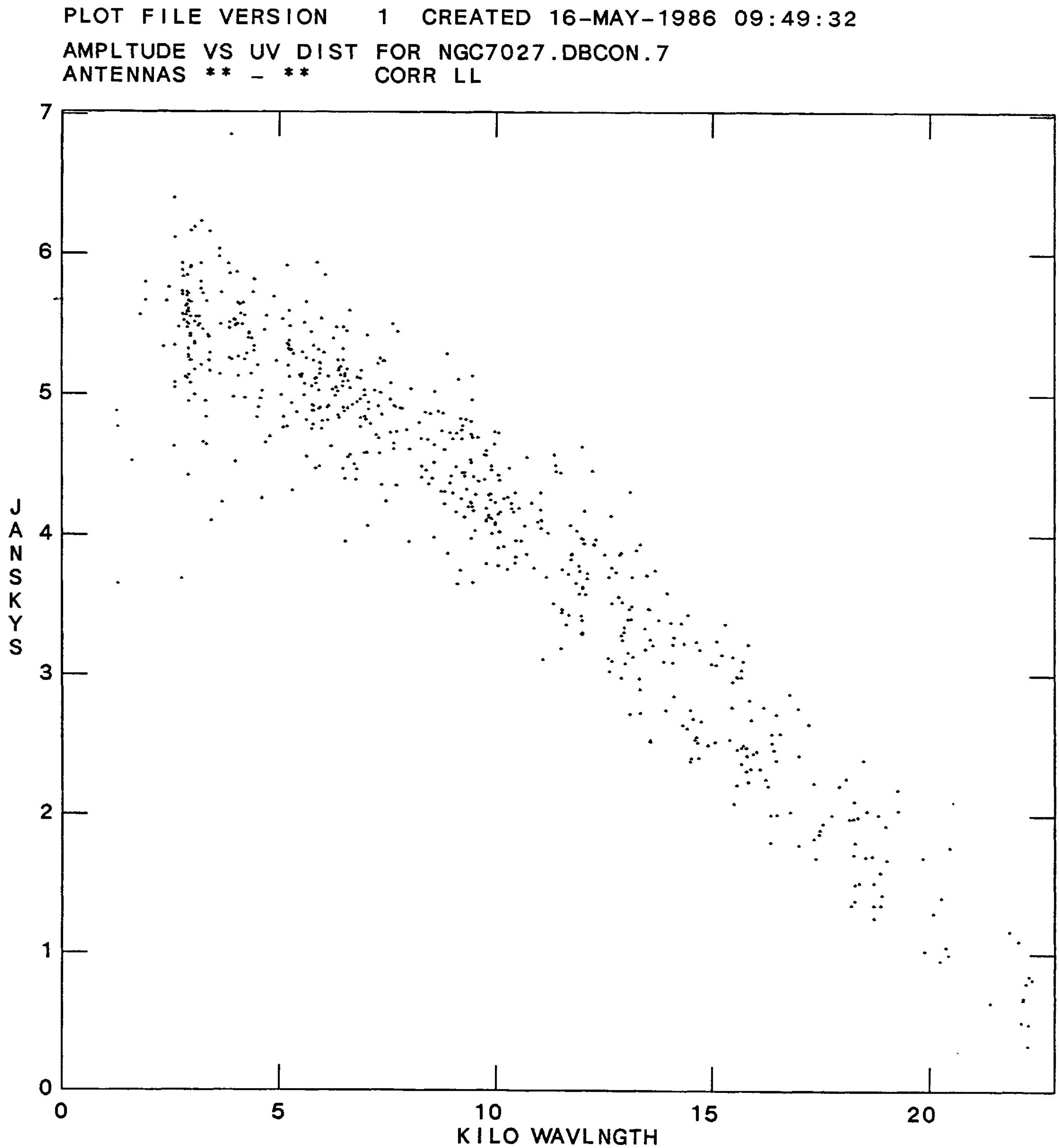
PLOT FILE VERSION 1 CREATED 16-MAY-1986 09:49:32
AMPLTUDE VS UV DIST FOR NGC7027.DBCON.7
ANTENNAS ** - ** CORR LL
JANSKYS
0
1
2
3
4
5
6
7
0
5
10
15
20
KILO WAVLNGTH

Figure 1.

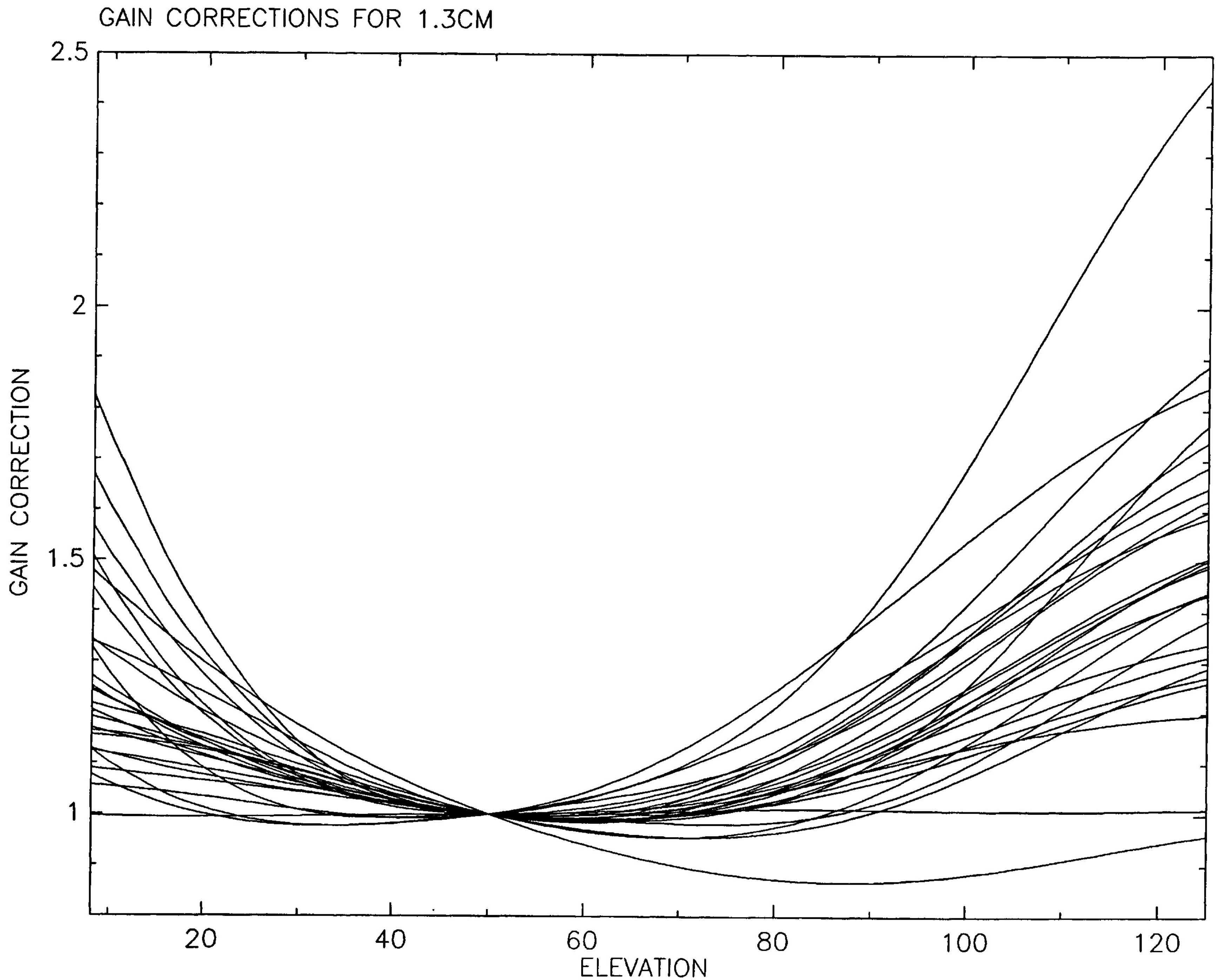
GAIN CORRECTIONS FOR 1.3CM
2.5
2
1.5
1
GAIN CORRECTION
20
40
60
80
100
120
ELEVATION

Figure 2.

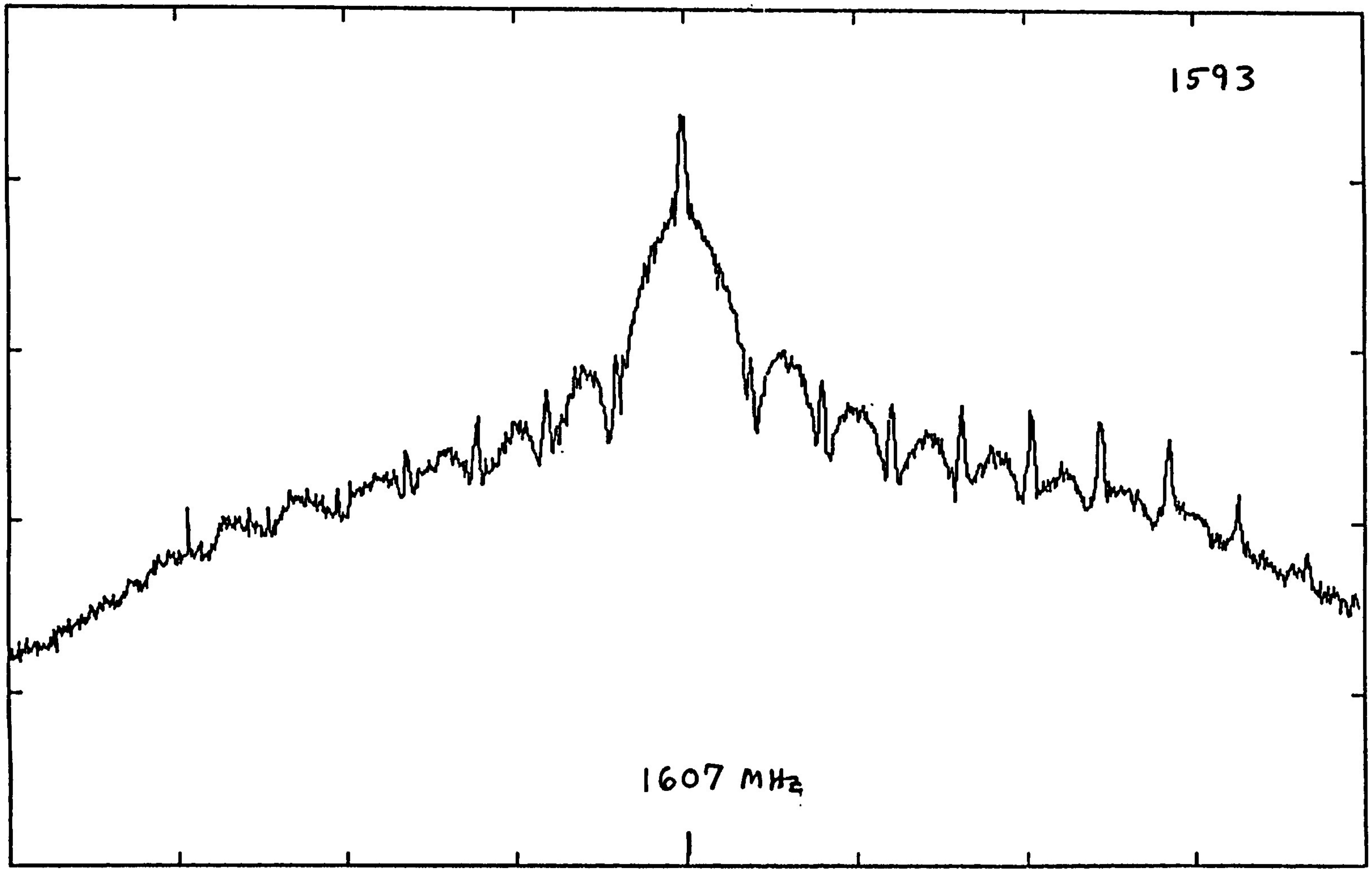

FIG. 3C

FIG. 4

COSMOS 1595

FREQUENCY = 1611.4 MHz.
AMPLITUDE = 29 db. (Above CASS A)

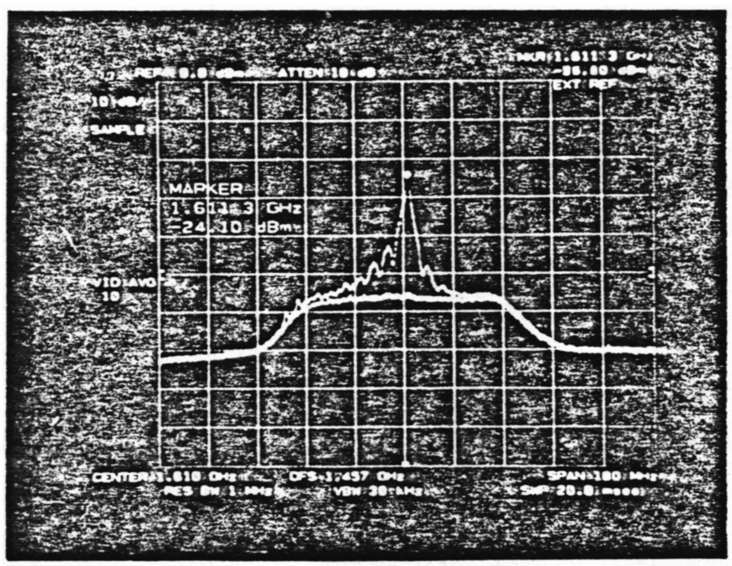

14

A. Center Freq. = 1610 MHz.
Freq. Span = 180 MHz.

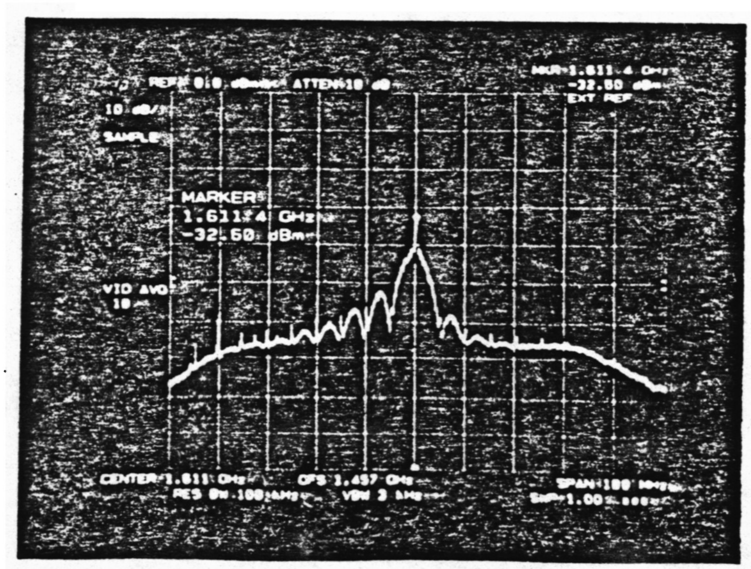

15

B. Center Freq. = 1611 MHz.
Freq. Span = 100 MHz.

FIG. 2

COSMOS 1520

FREQUENCY = 1615.3 MHz.
AMPLITUDE = 33 db. (Above CASS A)

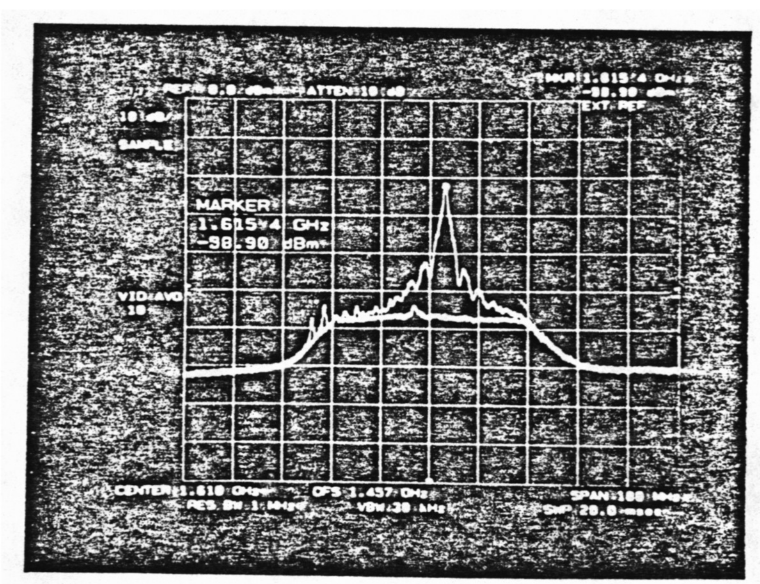

A. Center Freq. = 1610 MHz.
Freq. Span = 180 MHz.

2

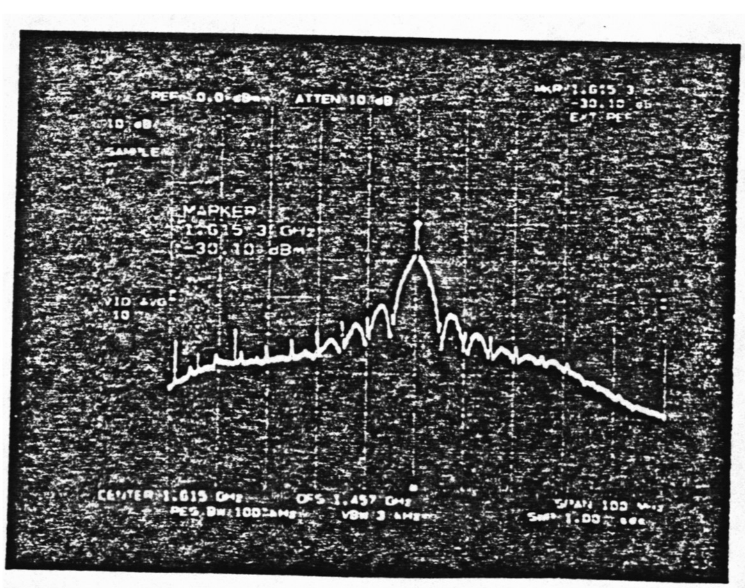

B. Center Freq. = 1615 MHz.
Freq. Span = 100 MHz.

3

FIG. 3

COSMOS 1593

FREQUENCY = 1607.4 MHz.
AMPLITUDE = 36 db. (Above CASS A)

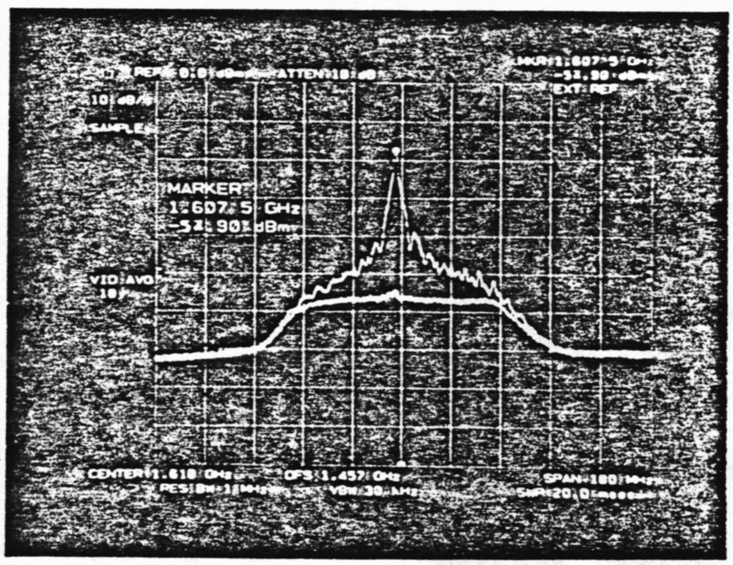

A. Center Freq. = 1610 MHz.
Freq. Span = 180 MHz.

12

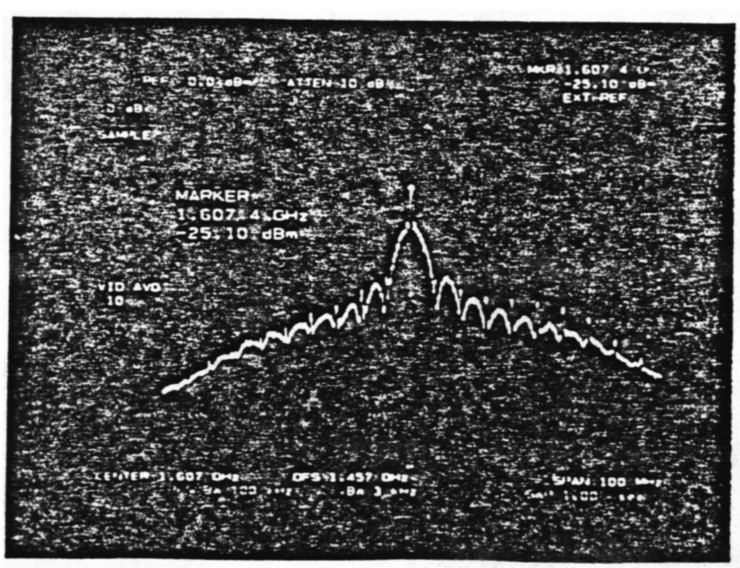

B. Center Freq. = 1607 MHz.
Freq. Span = 100 MHz.

13

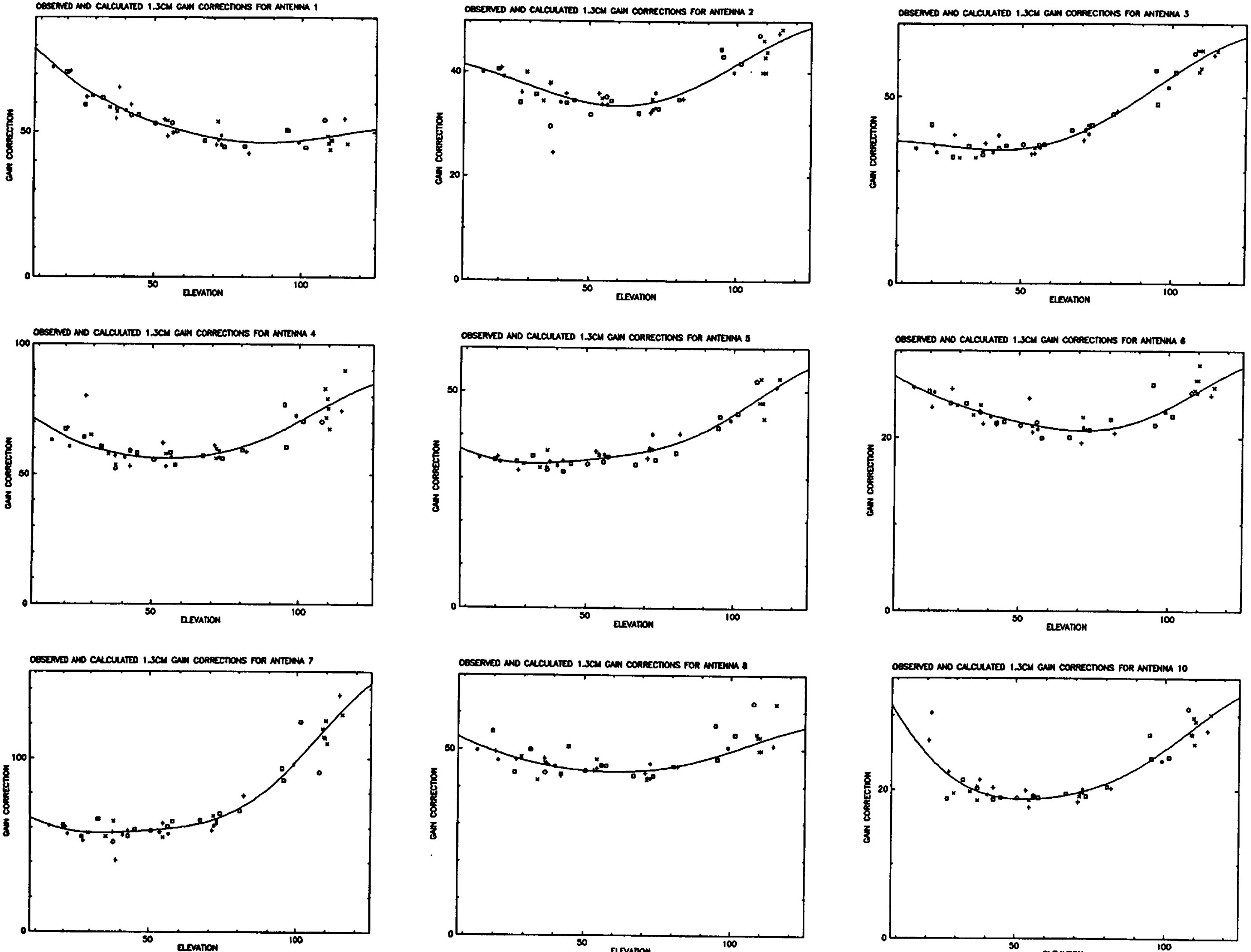

OBSERVED AND CALCULATED 1.3CM GAIN CORRECTIONS FOR ANTENNA 1
GAIN CORRECTION
ELEVATION
OBSERVED AND CALCULATED 1.3CM GAIN CORRECTIONS FOR ANTENNA 2
GAIN CORRECTION
ELEVATION
OBSERVED AND CALCULATED 1.3CM GAIN CORRECTIONS FOR ANTENNA 3
GAIN CORRECTION
ELEVATION
OBSERVED AND CALCULATED 1.3CM GAIN CORRECTIONS FOR ANTENNA 4
GAIN CORRECTION
ELEVATION
OBSERVED AND CALCULATED 1.3CM GAIN CORRECTIONS FOR ANTENNA 5
GAIN CORRECTION
ELEVATION
OBSERVED AND CALCULATED 1.3CM GAIN CORRECTIONS FOR ANTENNA 6
GAIN CORRECTION
ELEVATION
OBSERVED AND CALCULATED 1.3CM GAIN CORRECTIONS FOR ANTENNA 7
GAIN CORRECTION
ELEVATION
OBSERVED AND CALCULATED 1.3CM GAIN CORRECTIONS FOR ANTENNA 8
GAIN CORRECTION
ELEVATION
OBSERVED AND CALCULATED 1.3CM GAIN CORRECTIONS FOR ANTENNA 10
GAIN CORRECTION
ELEVATION

Figures 3-11.

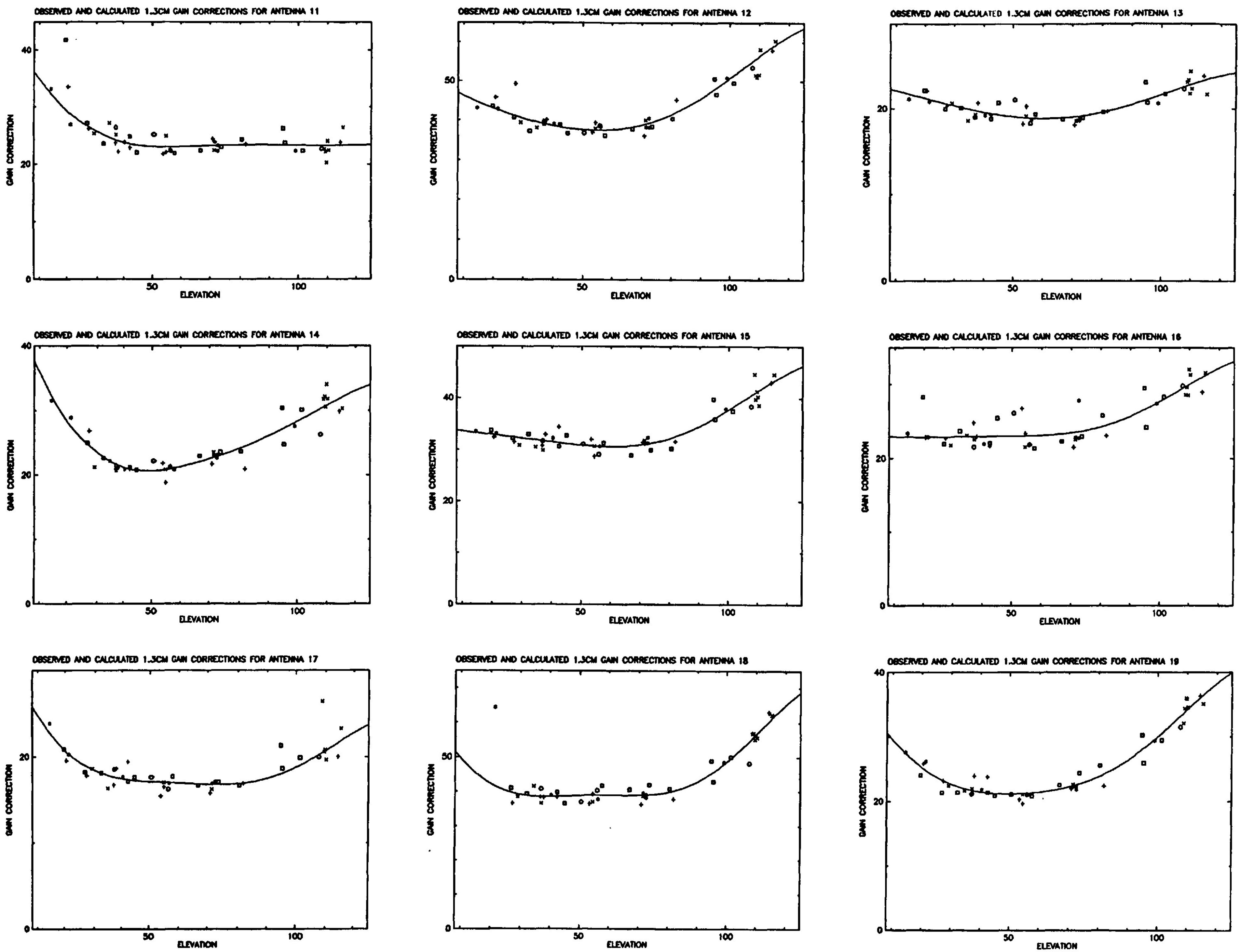

Figures 12-20.

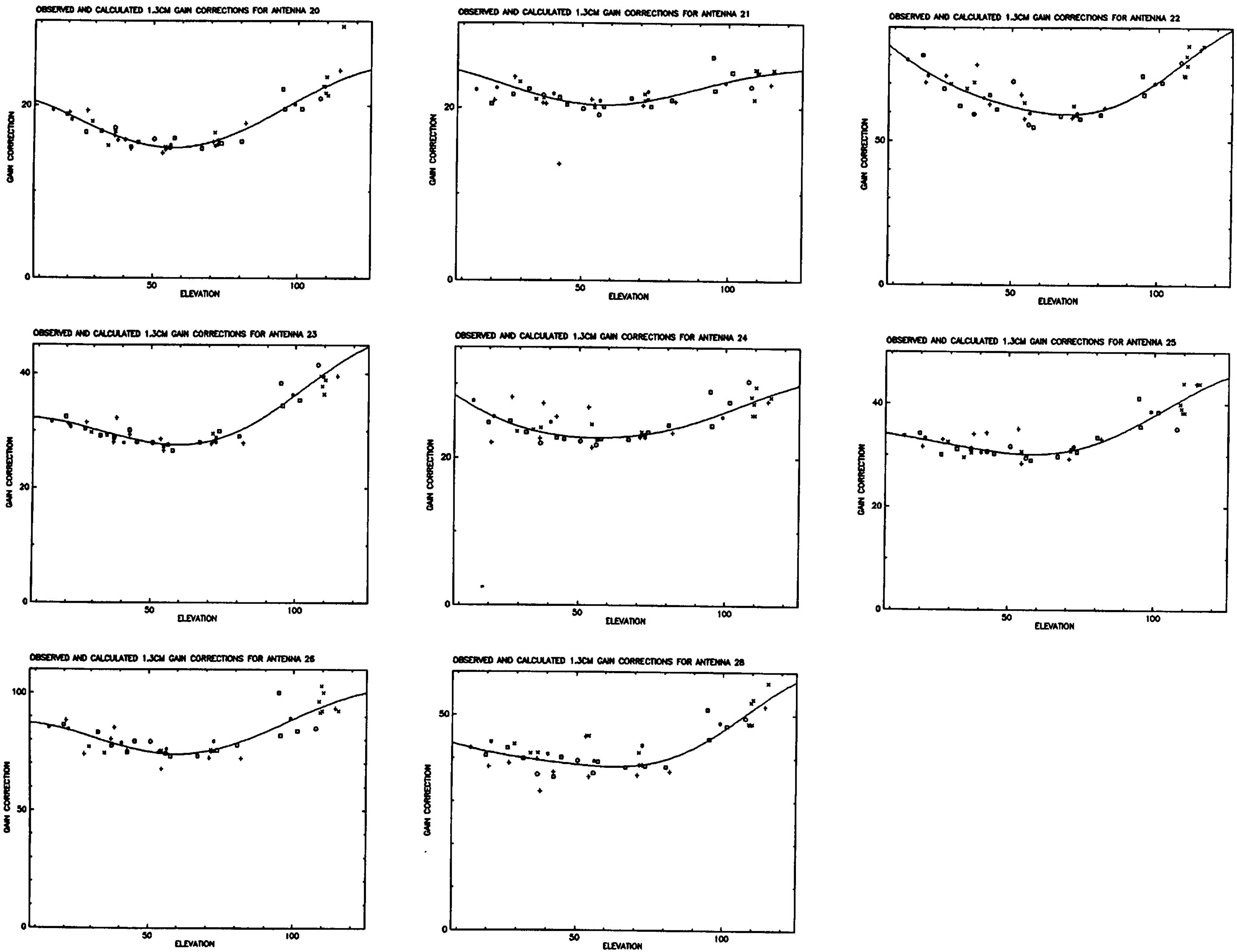

Figures 21-28.